










Assessment of Additional MRI-Detected Breast Lesions Using the Quantitative Analysis of Contrast-Enhanced Ultrasound Scans and Its Comparability with Dynamic Contrast-Enhanced MRI Findings of the Breast

유방자기공명영상에서 추가적으로 발견된 유방 병소에 대한 조영증강 초음파의 정량적 분석을 통한 진단 능력 평가와 동적 조영증강 유방 자기공명영상 결과와의 비교

Sei Young Lee, MD¹ , Ok Hee Woo, MD^{1*} , Hye Seon Shin, MD¹ ,
Sung Eun Song, MD² , Kyu Ran Cho, MD² ,
Bo Kyoung Seo, MD³ , Soon Young Hwang, PhD⁴ 

¹Department of Radiology, Korea University Guro Hospital, College of Medicine, Korea University, Seoul, Korea

²Department of Radiology, Korea University Anam Hospital, College of Medicine, Korea University, Seoul, Korea

³Department of Radiology, Korea University Ansan Hospital, College of Medicine, Korea University, Seoul, Korea

⁴Medical Science Research Support Center, Division of Medical Statistics, Korea University Guro Hospital, College of Medicine, Korea University, Seoul, Korea

Purpose To assess the diagnostic performance of contrast-enhanced ultrasound (CEUS) for additional MR-detected enhancing lesions and to determine whether or not kinetic pattern results comparable to dynamic contrast-enhanced magnetic resonance imaging (DCE-MRI) of the breast can be obtained using the quantitative analysis of CEUS.

Materials and Methods In this single-center prospective study, a total of 71 additional MR-detected breast lesions were included. CEUS examination was performed, and lesions were categorized according to the Breast Imaging-Reporting and Data System (BI-RADS). The sensitivity,

Received June 8, 2020
Revised September 4, 2020
Accepted September 14, 2020

*Corresponding author

Ok Hee Woo, MD
Department of Radiology,
Korea University Guro Hospital,
College of Medicine,
Korea University,
148 Gurodong-ro, Guro-gu,
Seoul 08308, Korea.








Tel 82-2-2626-1338

Fax 82-2-863-9282

E-mail wokhee@korea.ac.kr

This is an Open Access article distributed under the terms of the Creative Commons Attribution Non-Commercial License (<https://creativecommons.org/licenses/by-nc/4.0>) which permits unrestricted non-commercial use, distribution, and reproduction in any medium, provided the original work is properly cited.

ORCID iDs

Sei Young Lee 
<https://orcid.org/0000-0002-0758-944X>
Ok Hee Woo 
<https://orcid.org/0000-0003-3953-933X>
Hye Seon Shin 
<https://orcid.org/0000-0001-8569-4360>
Sung Eun Song 
<https://orcid.org/0000-0002-9259-8294>
Kyu Ran Cho 
<https://orcid.org/0000-0002-8936-6468>
Bo Kyoung Seo 
<https://orcid.org/0000-0002-9512-5361>
Soon Young Hwang 
<https://orcid.org/0000-0001-7474-1803>

specificity, and diagnostic accuracy of CEUS were calculated by comparing the BI-RADS category to the final pathology results. The degree of agreement between CEUS and DCE-MRI kinetic patterns was evaluated using weighted kappa.

Results On CEUS, 46 lesions were assigned as BI-RADS category 4B, 4C, or 5, while 25 lesions category 3 or 4A. The diagnostic performance of CEUS for enhancing lesions on DCE-MRI was excellent, with 84.9% sensitivity, 94.4% specificity, and 97.8% positive predictive value. A total of 57/71 (80%) lesions had correlating kinetic patterns and showed good agreement (weighted kappa = 0.66) between CEUS and DCE-MRI. Benign lesions showed excellent agreement (weighted kappa = 0.84), and invasive ductal carcinoma (IDC) showed good agreement (weighted kappa = 0.69).

Conclusion The diagnostic performance of CEUS for additional MR-detected breast lesions was excellent. Accurate kinetic pattern assessment, fairly comparable to DCE-MRI, can be obtained for benign and IDC lesions using CEUS.

Index terms Diagnostic Ultrasound; Contrast Media; Microbubbles; Magnetic Resonance Imaging; Breast Tumors; Breast Cancer

INTRODUCTION

Breast cancer is the most prevalent type of cancer among female worldwide, accounting for nearly one-fourth of all cancers (1). Breast magnetic resonance imaging (MRI) is a widely utilized modality for detection of breast cancer (2). It is also increasingly used for staging of known breast cancer and contralateral breast screening in newly diagnosed breast cancers. As a result, initially occult additional breast nodules are often detected on MRI (2).

However, the validity of MRI is limited by its specificity and moderate positive predictive value (PPV). In a prior meta-analysis of the role of pre-operative MRI in detection of unsuspected multifocal and/or multicentric cancer in the ipsilateral breast, the rate of detection of additional cancer foci ranged 6–34%, with a median of 16% and a PPV of 66% (3).

Therefore, when unsuspected additional MR-detected lesions can be correlated by second-look ultrasound (US), the more widely available technique of US-guided biopsy is recommended. However, the detection rate of second-look US is very heterogeneous due to the success of examination depending on the experience and technique of the operator (4). Furthermore, the low reproducibility of lesion characterization in breast US remains a problematic issue (4).

Contrast enhanced ultrasound (CEUS) has emerged as a popular diagnostic tool in evaluating breast lesions for malignancy (5). Breast cancers are closely associated with angiogenesis, which is the formation of new vascular network from preexisting vessels (1). Due to this fact, CEUS has become a useful tool for evaluating tumor microflow by using microbubble contrast agents (5, 6).

Compared with conventional US, CEUS can substantially improve visualization of the vascularity and parenchymal microcirculation within breast tumors by injection of microbubble-based contrast agents into a peripheral vein (7). Also, CEUS kinetic parameters can be quantitatively evaluated by a time-intensity curve (TIC) (8). Due to the advantage of providing both morphologic and functional information, CEUS has gained more and more attention in

recent studies (7, 8). Previous studies have also reported that CEUS enhancement patterns were useful in the prediction of breast cancer prognosis (8, 9).

In addition, quantitative analysis using CEUS also has several advantages over breast dynamic contrast enhanced MRI (DCE-MRI). DCE-MRI requires patient to be in prone position and uses contrast agents that are excreted through the renal system. CEUS is done in a relatively more comfortable supine position, and uses contrast agents that do not put renal function at risk (10). In addition, CEUS is able to dynamically observe the perfusion changes as opposed to multiple static images of DCE-MRI (11).

To our knowledge, current literature has no prospective results on the diagnostic performance of CEUS for additional MR-detected breast lesions using morphological and functional analysis. Also, comparison studies between breast DCE-MRI and CEUS kinetic pattern results has not been done.

The purpose of this study is to prospectively assess the diagnostic performance of CEUS for additional MR-detected enhancing breast lesions and to determine whether kinetic pattern results comparable to breast DCE-MRI can be obtained using quantitative analysis of CEUS.

MATERIALS AND METHODS

PATIENTS

This single center prospective study was approved by the Institutional Review Board and written informed consent was obtained (IRB No. 2015GR0724). From January 2016 to December 2018, 600 breast cancer patients scheduled for surgery underwent pre-operative breast MRI. There were 150 patients with additional MR-detected enhancing breast lesions, and among them, 71 lesions in 71 patients were correlated on 2nd look US exam. These seventy-one additional MR-detected lesions in 71 patients (mean age, 52.2 years; age range, 28–77 years) comprised the study group.

BREAST DCE-MRI EXAMINATION

All DCE-MRI images were obtained from pre-operative breast MR exam. Breast MRI was performed using a 3T MR scanner (MAGNETOM Skyra, Siemens Medical Solutions, Erlangen, Germany) in the prone position with their breasts placed in a dedicated 18-channel phased-array breast coil (Siemens Medical Solutions). Bilateral breast imaging was done with following protocol: an axial, turbo spin-echo T2-weighted sequence, diffusion weighted image sequence, and dynamic contrast-enhanced MRI (DCE-MRI) sequences. Contrast agent used was gadolinium-based and was administered through peripheral veins.

CEUS EXAMINATION

A single highly experienced radiologist performed the US exam with EPIQ 7 (Philips Healthcare, Bothell, WA, USA) unit and a 7.5–15 MHz linear transducer. First, the conventional US features including shape, orientation, margin, echogenicity, and posterior feature were evaluated. For CEUS, the machine parameters were set at mechanical index less than 0.1 and gain at 100–120 dB. No parameter changes were made during the examination.

The contrast agent used in this study was SonoVue (Bracco, Milan, Italy). About 3 mL of con-

trast agent was injected via peripheral vein in the arm in a bolus fashion and was followed by normal saline injection. Continuous imaging was done immediately after the injection and lasted for 3 minutes. The quantitative data acquisition for kinetic pattern assessment was done. During the exam, the selected plane was unchanged with the probe stabilized manually. The recorded images were stored in a hard disc on US machine for subsequent analysis. CEUS analysis was done with commercially available software (ViewBox; Bracco, Geneva, Switzerland)

IMAGE ANALYSIS

Two experienced radiologists reviewed all the DCE-MRI and CEUS images of 71 lesions until consensus was achieved. Both were blinded to patient's clinical information. The assessment of DCE-MRI and CEUS was based on our clinical experience and previous literatures (12, 13).

For each lesion, benign and malignant features on conventional US, CEUS, and DCE-MRI was evaluated. Malignant features included the following findings; irregular US shape, non-parallel US orientation, indistinct, angular, or spiculated US margin, hypoechoic or heterogeneous US echogenicity, posterior shadowing on US, peripheral CEUS enhancement, washout CEUS kinetics, irregular MRI shape, irregular or spiculated MRI margin, washout DCE-MRI kinetics, and heterogeneous DCE-MRI enhancement. Benign features include round or oval US shape, parallel US orientation, circumscribed US margin, isoechoic or hyperechoic US echogenicity, central CEUS enhancement, persistent CEUS kinetics, round or oval MRI shape, circumscribed MRI margin, persistent DCE-MRI kinetics, and homogeneous DCE-MRI enhancement.

The kinetic pattern for both DCE-MRI and CEUS was obtained using quantitative parameters of the TIC generated by built-in software and Viewbox. The patterns were categorized into persistent, plateau, or washout for both DCE-MRI and CEUS.

Each of the 71 lesions was categorized according to BI-RADS using combination of conventional US and CEUS features with priority given to CEUS features when categorizing them into BI-RADS. BI-RADS category 3 and 4A were considered as benign, and category 4B, 4C, and 5 were considered malignant for the calculation of CEUS diagnostic efficacy.

HISTOPATHOLOGIC ANALYSIS

All histopathologic analysis was performed in consensus by two experienced pathologists. The diagnosis of the additional MR-detected lesions was confirmed at histopathologic examination of the specimens obtained by either surgical resection or core needle biopsy.

STATISTICAL ANALYSIS

All statistical analysis was performed with statistical software (version 18.5., Medcalc for windows; Ostend, Belgium).

The diagnostic performance of CEUS was analyzed by comparing CEUS BI-RADS category to reference standard histopathology results. Sensitivity, specificity, PPV, and area under the curve (AUC) were calculated.

Correlation of various CEUS and DCE-MRI features with malignancy was analyzed using

Fisher exact test. The level of statistical significance was set at *p* value less than 0.05.

The degree of agreement between kinetic patterns of DCE-MRI and CEUS was analyzed by using weighted kappa analysis. Weighted kappa values were interpreted as follows; 0–0.2 poor, 0.21–0.4 fair, 0.41–0.6 moderate, 0.61–0.8 good, and 0.81–1.0 excellent (14).

RESULTS

Of the 71 US-correlated additional MRI-detected lesions, 53 (75%) lesions were malignant and 18 (25%) were benign. Among the 53 malignant lesions, there were 37 (71%) invasive ductal carcinoma (IDC), 8 (15%) ductal carcinoma in situ (DCIS), 7 (13%) invasive lobular carcinoma (ILC), and 1 (0.5%) mucinous carcinoma (Table 1). The size of these lesions were as follows; 0–0.5 cm (*n* = 6), 0.5–1 cm (*n* = 44), 1–1.5 cm (*n* = 14), 1.5–2 cm (*n* = 4), 2–2.5 cm (*n* = 2), over 2.5 cm (*n* = 1).

DIAGNOSTIC PERFORMANCE OF CEUS

There were 46 lesions categorized as BI-RADS 4B, 4C, or 5 by CEUS, and 45/46 lesions were confirmed as malignant or true positive. Twenty-five lesions were categorized as BI-RADS 3 or 4A by CEUS, and 17/25 lesions were confirmed as benign or true negative. The sensitivity and specificity was 84.9% and 94.4%, respectively. AUC was 0.897 and PPV was 97.8% (Table 2).

ASSOCIATION BETWEEN VARIOUS CEUS/DCE-MRI FEATURES AND MALIGNANCY

There was statistically significant association between malignancy and the following features; CEUS enhancement pattern, CEUS kinetic pattern, US shape, US margin, US echo, MRI

Table 1. Histopathology Results of Additional MR-Detected Lesions

Lesion Pathology	Number (%)
Malignant	53 (75)
IDC	37 (70)
ILC	8 (15)
DCIS	7 (13)
Mucinous carcinoma	1 (2)
Benign	18 (25)
Total	71 (100)

DCIS = ductal carcinoma in situ, IDC = invasive ductal carcinoma, ILC = invasive lobular carcinoma

Table 2. Prospective Diagnostic Performance of Contrast-Enhanced Ultrasound for Second-Look Lesions

Measure	Estimate
Sensitivity (%)	84.91
Specificity (%)	94.44
Positive predictive value (%)	97.83
Negative predictive value (%)	68.00
Area under the curve	0.897

Table 3. Association between CEUS/Dynamic Contrast-Enhanced MRI Features and Malignancy

Feature	Number	p-Value
CEUS enhancement pattern		0.0005
Central	23	
Peripheral*	48	
CEUS kinetic		0.0001
Persistent	10	
Plateau	13	
Washout*	48	
US shape		0.0002
Round	2	
Oval	22	
Irregular*	47	
US orientation		0.07
Parallel	49	
Non-parallel*	21	
US margin		0.0018
Circumscribed	20	
Indistinct*	34	
Angular*	6	
Spiculated*	11	
US echogenicity		0.0173
Hypoechoic*	56	
Hyper or isoechoic	12	
Heterogeneous	2	
US posterior feature		0.17
None	62	
Shadowing*	8	
Enhancement	1	
MRI enhancement pattern		< 0.0001
Homogeneous	17	
Heterogeneous*	48	
Rim*	6	
MRI kinetic		< 0.0115
Persistent	19	
Plateau	15	
Washout*	37	
MRI shape		0.0001
Round	5	
Oval	24	
Irregular*	38	
NME [†]	4	
MRI margin		< 0.0001
Circumscribed	25	
Irregular*	31	
Spiculated*	11	
NME [†]	4	

*Malignant features.

[†] Four NME lesions on MRI were visualized as a mass morphology on US.

CEUS = contrast-enhanced ultrasound, NME = non-mass enhancement, US = ultrasound

enhancement pattern, MR kinetic pattern, MR shape, and MR margin (all p value < 0.05) (Table 3). US orientation and posterior features were not significantly associated with malignancy ($p = 0.07$ and $p = 0.17$, respectively).

KINETIC PATTERN AGREEMENT BETWEEN CEUS AND DCE-MRI

Overall, 56/70 (80%) evaluated lesions showed the same kinetic patterns between the two modalities. The degree of agreement of kinetic patterns between CEUS and DCE-MRI was good (weighted kappa = 0.66) (Table 4). The total number and percentage of benign and malignant lesions showing various kinetic patterns can be seen on Table 5.

For benign lesions, 16/18 (89%) nodules had correlating kinetic patterns between CEUS and DCE-MRI. The degree of agreement was excellent with weighted kappa value of 0.84 (Table 4). The 2 lesions that did not show the same kinetic pattern had persistent curve on DCE-MRI and plateau curve on CEUS. All lesions that showed plateau or washout curves on DCE-MRI had the same pattern on CEUS. An example of a benign lesion showing the same persistent kinetic pattern in DCE-MRI and CEUS can be seen in Fig. 1.

For malignant lesions, 40/52 (77%) lesions displayed the same kinetic patterns on both DCE-MRI and CEUS. The calculated weighted kappa value was 0.38, showing fair agreement (Table 4). For malignant lesions showing washout patterns, all of them had same kinetic patterns between CEUS and DCE-MRI (35/35, 100%). Persistent and plateau patterns in malignant lesions were poorly matched between the two modalities (6/18, 33%).

Table 4. Kinetic Pattern Agreement between Contrast-Enhanced Ultrasound and Dynamic Contrast-Enhanced MRI for Additional MR-Detected Lesions

Lesion Pathology	Agreement (%)	Weighted Kappa Value
Total	56/70 (80)	0.66 (good)
Benign	16/18 (89)	0.84 (excellent)
Malignant	40/52 (77)	0.38 (fair)
IDC	34/37 (92)	0.69 (good)
DCIS	3/8 (38)	0.13 (poor)
ILC	3/7 (43)	0.15 (poor)

DCIS = ductal carcinoma in situ, IDC = invasive ductal carcinoma, ILC = invasive lobular carcinoma

Table 5. Kinetic Patterns on CEUS and DCE-MRI for Additional MR-Detected Lesions

	Benign Lesion Number (%)	Malignant Lesion Number (%)
CEUS kinetics		
Persistent	9 (50)	1 (2)
Plateau	7 (39)	5 (10)
Washout	2 (11)	46 (88)
DCE-MRI kinetics		
Persistent	11 (61)	8 (15)
Plateau	5 (28)	10 (19)
Washout	2 (11)	34 (65)
Total	18	52

CEUS = contrast-enhanced ultrasound, DCE = dynamic contrast-enhanced

Fig. 1. A benign lesion, confirmed as usual ductal hyperplasia, in a 76-year-old female shows kinetic pattern agreement between CEUS and DCE-MRI.

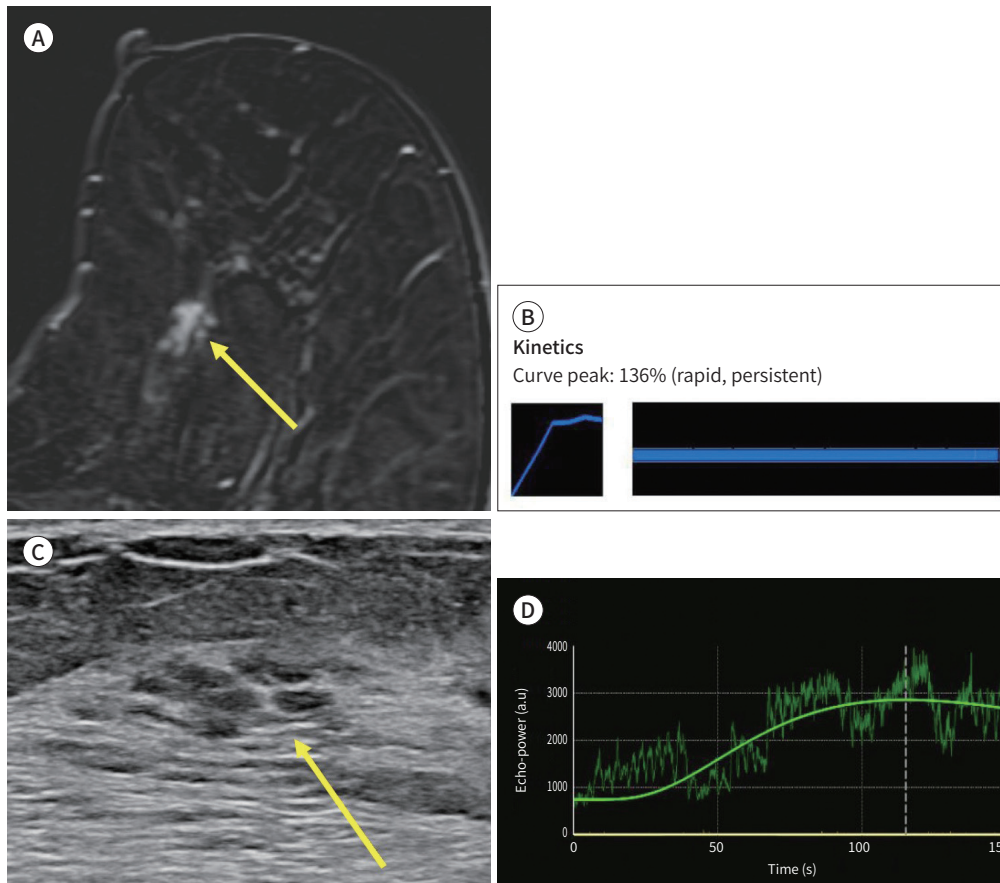
A. An enhancing lesion in the 10 o'clock portion of the left breast is noted on preoperative breast DCE-MRI (yellow arrow).

B. Computer-aided detection for the quantitative kinetic pattern analysis of the lesion shows a type 1 persistent kinetic curve.

C. This additional MR-detected enhancing lesion in the 10 o'clock portion of the left breast correlates on second-look ultrasound (yellow arrow).

D. The quantitative kinetic pattern analysis of the second-look lesion on CEUS shows a type 1 persistent kinetic curve.

CEUS = contrast-enhanced ultrasound, DCE = dynamic contrast-enhanced



In a subgroup analysis of different cancer types, 34/37 (92%) of IDC lesions showed good agreement (weighted kappa = 0.69), 3/8 (38%) DCIS lesions showed poor agreement (weighted kappa = 0.13), and 3/7 (43%) ILC lesions showed poor agreement (weighted kappa = 0.15) (Table 4). An example of IDC lesion showing the same washout kinetic pattern in DCE-MRI and CEUS can be seen in Fig. 2. Examples of ILC and DCIS lesions showing different kinetic patterns can be seen in Fig. 3 and Fig. 4, respectively.

DISCUSSION

Breast MRI is regarded as an important diagnostic tool for the detection of unsuspected breast lesions (15). Because of MRI's low specificity, tissue confirmation is often required,

Fig. 2. An invasive ductal carcinoma lesion in a 56-year-old female shows a kinetic pattern agreement between CEUS and DCE-MRI.

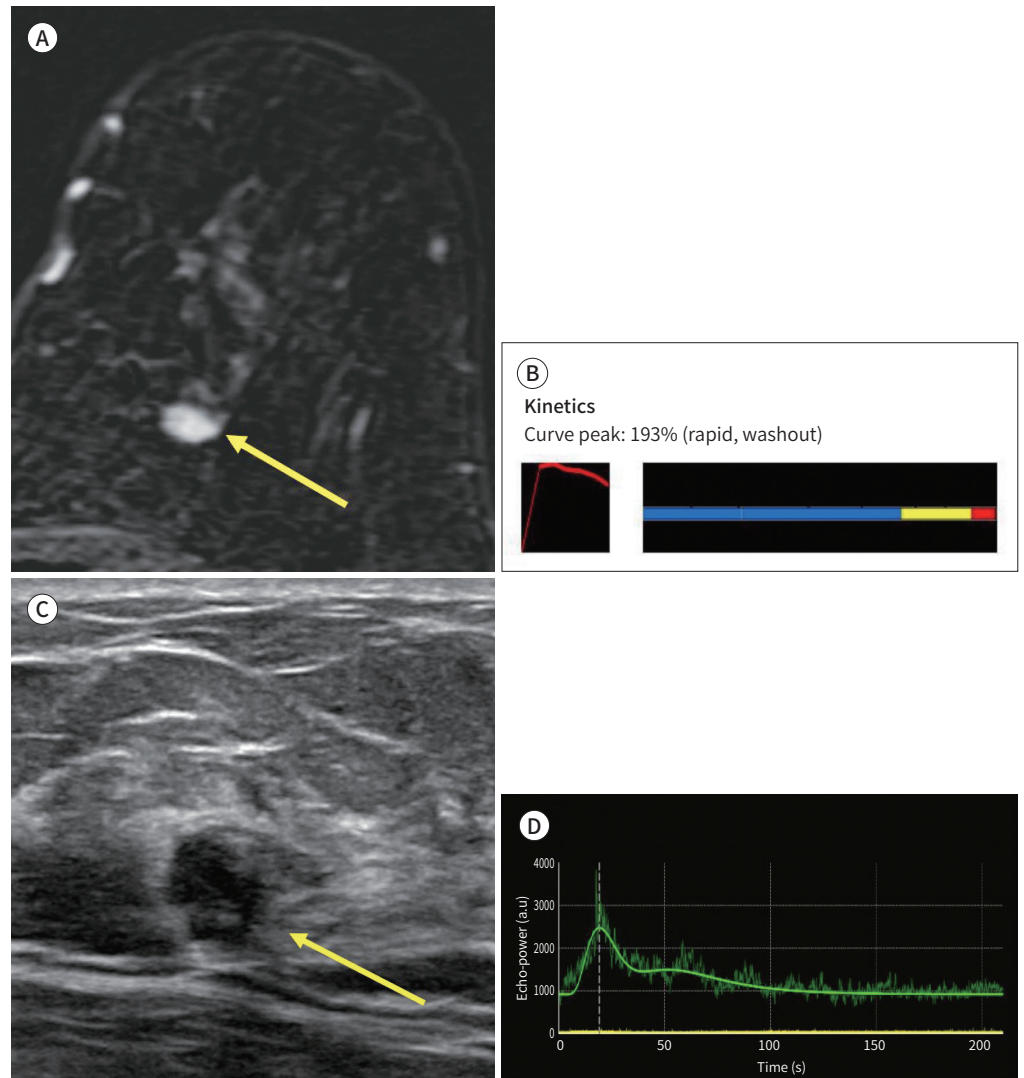
A. An enhancing lesion in the 10 o'clock portion of the left breast is noted on preoperative breast DCE-MRI (yellow arrow).

B. Computer-aided detection for the quantitative kinetic pattern analysis of the lesion shows a type 3 washout kinetic curve.

C. This additional MR-detected enhancing lesion in the 10 o'clock portion of the left breast correlates on second-look ultrasound (yellow arrow).

D. The quantitative kinetic pattern analysis of the second-look lesion on CEUS shows a type 3 washout kinetic curve.

CEUS = contrast-enhanced ultrasound, DCE = dynamic contrast-enhanced



and second-look evaluation is usually done with conventional US (15). However, conventional US has its downfalls due to heterogeneous detection rate depending on the operator (4).

Our study prospectively showed that the diagnostic performance of CEUS, which utilizes morphological and functional analysis, was excellent in differentiating benign from malignant additional MR-detected breast lesions. AUC value was 0.897 in this study and is comparable to AUC of 0.841 in another prospective CEUS study done for differentiating benign from

Fig. 3. An invasive lobular carcinoma lesion in a 58-year-old female shows kinetic pattern disagreement between CEUS and DCE-MRI.

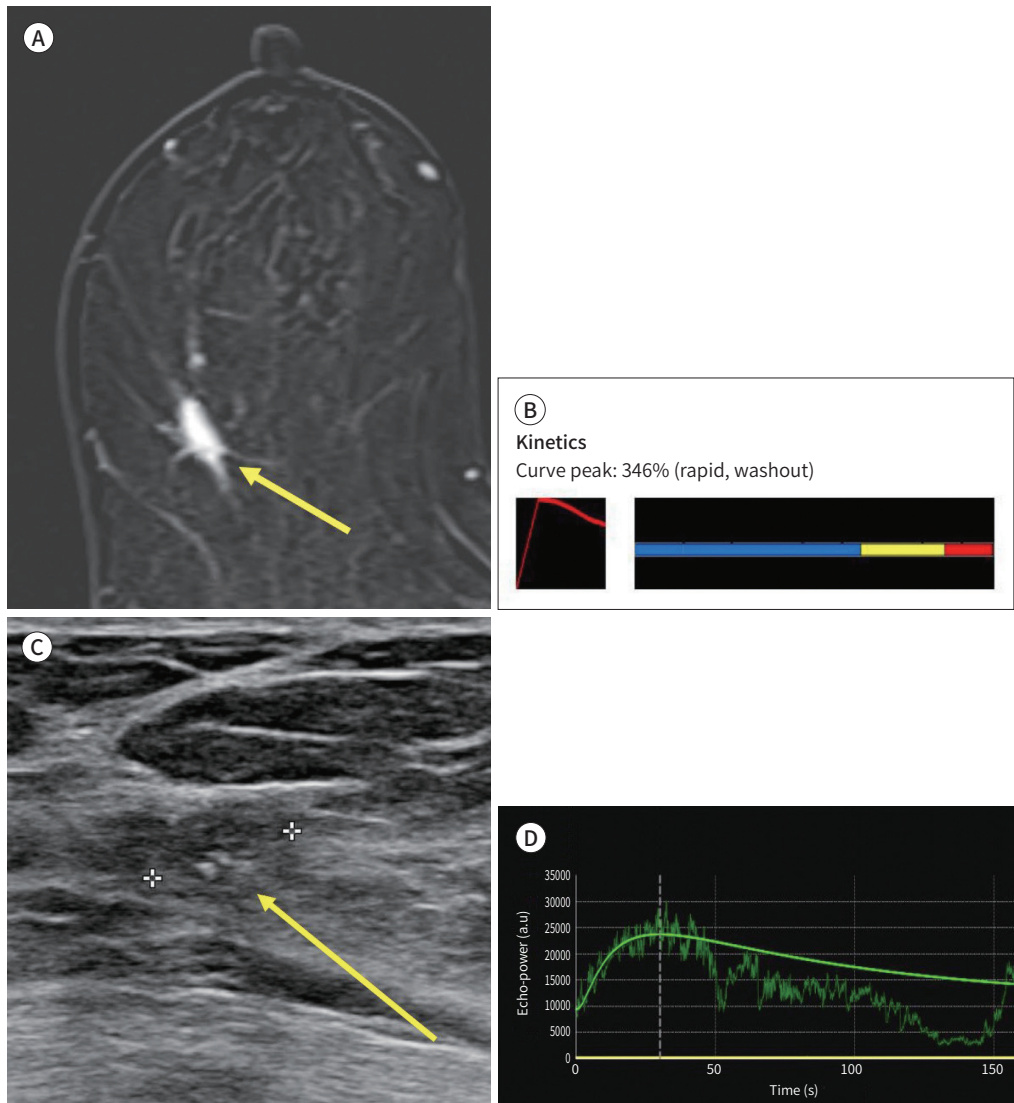
A. An enhancing lesion in the 9 o'clock portion of the right breast is noted on preoperative breast DCE-MRI (yellow arrow).

B. Computer aided detection for the quantitative kinetic pattern analysis of the lesion shows a type 3 wash-out kinetic curve.

C. This additional MR-detected enhancing lesion in the 9 o'clock portion of the right breast correlates on second-look ultrasound (yellow arrow).

D. The quantitative kinetic pattern analysis of the second-look lesion on CEUS shows a type 2 plateau kinetic curve.

CEUS = contrast-enhanced ultrasound, DCE = dynamic contrast-enhanced



malignant masses (16). CEUS features of malignant masses include heterogeneous enhancement, centripetal enhancement, early strong enhancement, penetrating vessels, and perfusion defects (16, 17). Its quantitative analysis also provides TIC. These additional informations allow CEUS to significantly help in the diagnosis of additional MR-detected breast lesions.

Furthermore, previously reported prospective CEUS study performed with initially detect-

Fig. 4. A ductal carcinoma in situ lesion in a 53-year-old female shows kinetic pattern disagreement between CEUS and DCE-MRI.

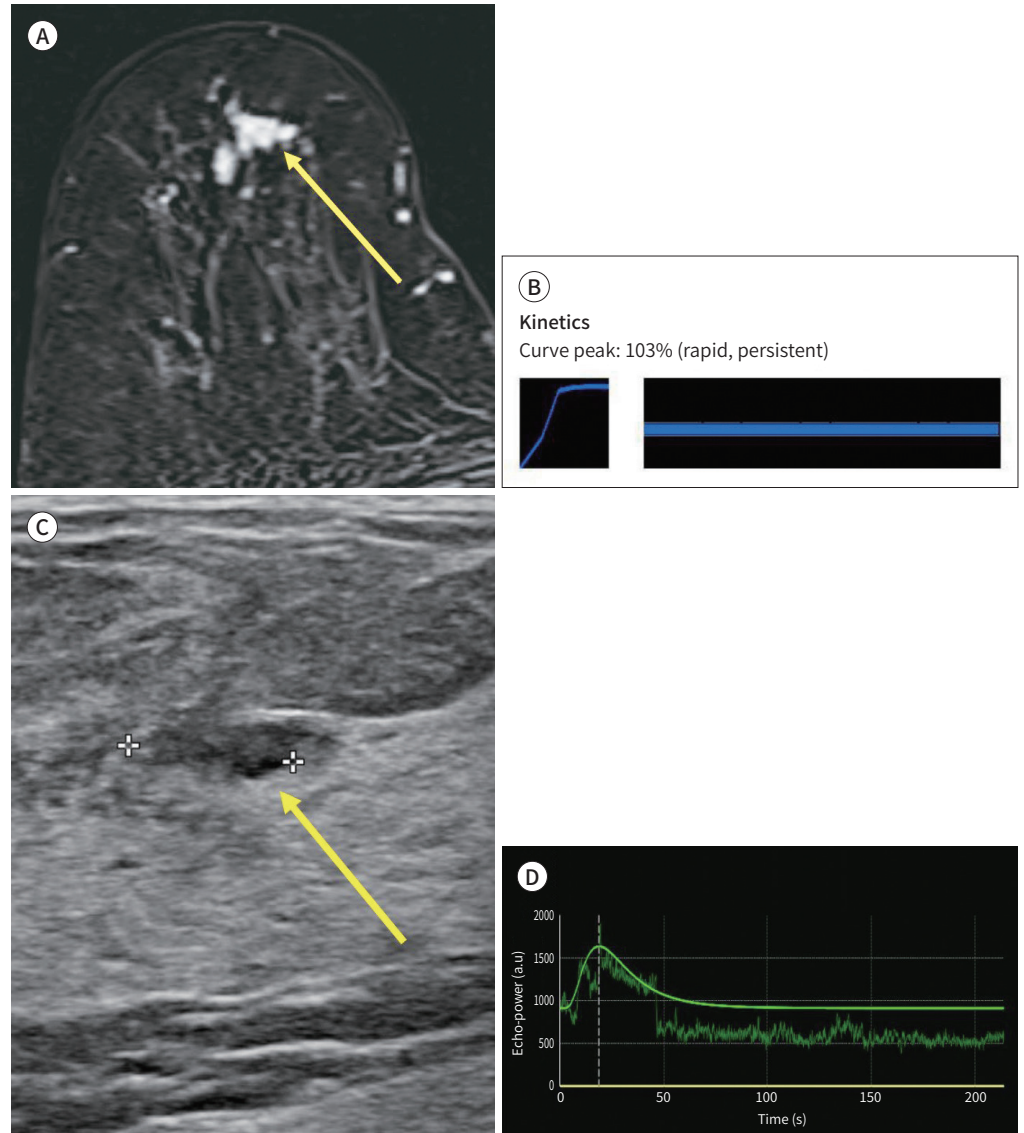
A. An enhancing lesion in the 12 o'clock portion of the right breast is noted on preoperative breast DCE-MRI (yellow arrow).

B. Computer-aided detection for the quantitative kinetic pattern analysis of the lesion shows a type 1 persistent kinetic curve.

C. This additional MR-detected enhancing lesion in the 12 o'clock portion of the right breast correlates on second-look ultrasound (yellow arrow).

D. The quantitative kinetic pattern analysis of the second-look lesion on CEUS shows a type 3 washout kinetic curve.

CEUS = contrast-enhanced ultrasound, DCE = dynamic contrast-enhanced



ed BI-RADS 4 and 5 lesions also showed good diagnostic performance in differentiating benign and malignant breast lesions (16). Together, these results show that morphological and functional analysis using CEUS for additional MR-detected breast lesions may provide added benefits in future clinical practice.

The CEUS and DCE-MRI features assessed for association with malignancy in this study

showed statistically significant association except for US orientation and posterior features. This may have resulted due to small lesion size of our study samples, which were entirely composed of additional MR-detected breast lesions.

Overall, there was good agreement between the kinetic patterns of DCE-MRI and CEUS for additional MR-detected lesions. This is probably because the majority of the evaluated lesions were composed of IDCs and benign lesions, which eventually displayed high degree of agreement between the two modalities in subgroup analyses.

There was poor agreement between kinetic patterns of DCE-MRI and CEUS for DCIS and ILC lesions. The discordance in DCIS may be attributed to the widely significant variability of MR enhancement kinetics of DCIS which display all persistent, plateau, and washout patterns (18). DCIS also predominantly exhibits non-mass morphology with clumped or heterogeneous enhancement with segmental or linear distribution (19). This nature of DCIS may also have contributed to poor agreement by posing technical difficulties in drawing reliable regions of interest (ROIs) for kinetic pattern assessment on CEUS. More than half of DCIS lesions were composed of NMEs in our study.

As for ILC lesions, the poor agreement may be attributed to low blood vessel permeability and variable microvasculature (20). ILC shows markedly lower expression of vascular endothelial growth factor (VEGF) (also known as vascular permeability factor) compared to IDC, resulting in relatively slower enhancement and longer time-to-peak (20). This slow enhancement where permeability of vessels in tumor and normal breast tissue are nearly same, may have led to different kinetic patterns depending on the modality. VEGF also contributes to angiogenesis and lower levels of expression may lead to variable microvasculature in ILC (20).

The poor agreement of persistent and plateau kinetic enhancement patterns compared to washout patterns among malignant lesions is probably due to large proportion of these type 1 and 2 curves being seen in ILC and DCIS lesions.

There were several limitations in our study. First, the study sample size was small. However, due to this study being a prospective investigation, results may still be a meaningful step for further research. Second, manual selection of ROIs on CEUS kinetic assessment may have led to inconsistent results. Lastly, CEUS image interpretation was done in consensus by two radiologists instead of performing individual analysis with inter-observer agreement, which may have improved the reliability. However, because there aren't established standardized protocol of interpreting CEUS images, consensus agreement was done.

In conclusion, prospectively evaluated diagnostic performance of CEUS for additional MR-detected breast lesions was excellent. Accurate kinetic pattern assessment that is fairly comparable to DCE-MRI can be obtained for benign and IDC lesions by using CEUS. Therefore, CEUS may have added value in clinical practice by providing alternative method of assessment in preoperative breast cancer patients with additionally detected lesions.

Author Contributions

Conceptualization, S.H.S., W.O.H.; data curation, L.S.Y., S.H.S., W.O.H.; formal analysis, L.S.Y., S.H.S., W.O.H., H.S.Y.; investigation, L.S.Y., S.H.S., W.O.H.; methodology, S.H.S., W.O.H.; project administration, W.O.H.; resources, L.S.Y., S.H.S., W.O.H.; supervision, W.O.H.; writing—original draft, L.S.Y.; and writing—review & editing, L.S.Y., W.O.H., S.H.S., S.S.E., C.K.R., S.B.K.

Conflicts of Interest

The authors have no potential conflicts of interest to disclose.

Funding

None

REFERENCES

1. Sridharan A, Eisenbrey JR, Dave JK, Forsberg F. Quantitative nonlinear contrast-enhanced ultrasound of the breast. *AJR Am J Roentgenol* 2016;207:274-281
2. Kuhl CK. Current status of breast MR imaging. Part 2. Clinical applications. *Radiology* 2007;244:672-691
3. Houssami N, Ciatto S, Macaskill P, Lord SJ, Warren RM, Dixon JM, et al. Accuracy and surgical impact of magnetic resonance imaging in breast cancer staging: systematic review and meta-analysis in detection of multifocal and multicentric cancer. *J Clin Oncol* 2008;26:3248-3258
4. Spick C, Baltzer PA. Diagnostic utility of second-look US for breast lesions identified at MR imaging: systematic review and meta-analysis. *Radiology* 2014;273:401-409
5. Wan C, Du J, Fang H, Li F, Wang L. Evaluation of breast lesions by contrast enhanced ultrasound: qualitative and quantitative analysis. *Eur J Radiol* 2012;81:e444-e450
6. Chung YE, Kim KW. Contrast-enhanced ultrasonography: advance and current status in abdominal imaging. *Ultrasonography* 2015;34:3-18
7. Moon WK, Im JG, Noh DY, Han MC. Nonpalpable breast lesions: evaluation with power Doppler US and a microbubble contrast agent-initial experience. *Radiology* 2000;217:240-246
8. Wan CF, Du J, Fang H, Li FH, Zhu JS, Liu Q. Enhancement patterns and parameters of breast cancers at contrast-enhanced US: correlation with prognostic factors. *Radiology* 2012;262:450-459
9. Wang Z, Zhou Q, Liu J, Tang S, Liang X, Zhou Z, et al. Tumor size of breast invasive ductal cancer measured with contrast-enhanced ultrasound predicts regional lymph node metastasis and N stage. *Int J Clin Exp Pathol* 2014;7:6985-6991
10. Nykänen A, Arponen O, Sutela A, Vanninen R, Sudah M. Is there a role for contrast-enhanced ultrasound in the detection and biopsy of MRI only visible breast lesions? *Radiol Oncol* 2017;51:386-392
11. Sun F, Cui L, Zhang L, Hao J, Gu J, Du J, et al. Intravesical contrast-enhanced ultrasound (CEUS) for the diagnosis of vesicouterine fistula (VUF): a case report. *Medicine (Baltimore)* 2018;97:e0478
12. Zhao H, Xu R, Ouyang Q, Chen L, Dong B, Huihua Y. Contrast-enhanced ultrasound is helpful in the differentiation of malignant and benign breast lesions. *Eur J Radiol* 2010;73:288-293
13. Tuncbilek N, Unlu E, Karakas HM, Cakir B, Ozyilmaz F. Evaluation of tumor angiogenesis with contrast-enhanced dynamic magnetic resonance mammography. *Breast J* 2003;9:403-408
14. Cohen J. Weighted kappa: nominal scale agreement with provision for scaled disagreement or partial credit. *Psychol Bull* 1968;70:213-220
15. Orel SG, Schnall MD. MR imaging of the breast for the detection, diagnosis, and staging of breast cancer. *Radiology* 2001;220:13-30
16. Park AY, Kwon M, Woo OH, Cho KR, Park EK, Cha SH, et al. A prospective study on the value of ultrasound microflow assessment to distinguish malignant from benign solid breast masses: association between ultrasound parameters and histologic microvessel densities. *Korean J Radiol* 2019;20:759-772
17. Du J, Wang L, Wan CF, Hua J, Fang H, Chen J, et al. Differentiating benign from malignant solid breast lesions: combined utility of conventional ultrasound and contrast-enhanced ultrasound in comparison with magnetic resonance imaging. *Eur J Radiol* 2012;81:3890-3899
18. Jansen SA, Newstead GM, Abe H, Shimauchi A, Schmidt RA, Karczmar GS. Pure ductal carcinoma in situ: kinetic and morphologic MR characteristics compared with mammographic appearance and nuclear grade. *Radiology* 2007;245:684-691
19. Mossa-Basha M, Fundaro GM, Shah BA, Ali S, Pantelic MV. Ductal carcinoma in situ of the breast: MR imaging findings with histopathologic correlation. *Radiographics* 2010;30:1673-1687
20. Mann RM, Veltman J, Huisman H, Boetes C. Comparison of enhancement characteristics between invasive lobular carcinoma and invasive ductal carcinoma. *J Magn Reson Imaging* 2011;34:293-300

유방자기공명영상에서 추가적으로 발견된 유방 병소에 대한 조영증강 초음파의 정량적 분석을 통한 진단 능력 평가와 동적 조영증강 유방 자기공명영상 결과와의 비교

이세영¹ · 우옥희^{1*} · 신혜선¹ · 송성은² · 조규란² · 서보경³ · 황순영⁴

목적 자기공명영상에서 추가적으로 발견된 조영증강 병소에 대한 조영증강 초음파의 진단 능력을 평가하고 조영증강 초음파의 정량 분석을 사용하여 유방 동적 조영증강 자기공명영상과 유사한 운동 패턴 결과를 얻을 수 있는지 분석하였다.

대상과 방법 단일 센터 전향적 연구로 진행하였고, 총 71개의 자기공명영상에서 추가적으로 발견된 조영증강 병소가 포함되었다. 이러한 병소에 대해 조영증강 초음파를 시행하였고 Breast Imaging-Reporting and Data System (이하 BI-RADS)에 따라 분류하였다. 그리고 모든 병소의 BI-RADS 분류를 조직학적 결과와 비교하여 조영증강 초음파의 민감도, 특이도 및 진단 정확도를 계산하였다. 조영증강 초음파와 동적 조영증강 자기공명영상의 운동 패턴 사이의 일치도는 가중 카파 분석을 사용하여 평가되었다.

결과 조영증강 초음파에서 총 46개의 병소가 BI-RADS 4B, 4C, 5로 분류되었고, 25개의 병소가 BI-RADS 3, 4A로 분류되었다. 자기공명영상에서 추가적으로 발견된 조영증강 병소에 대한 조영증강 초음파의 진단 능력은 84.9%의 민감도, 94.4%의 특이도 및 97.8%의 긍정적 예측값으로 우수하였다. 총 57/71 (80%) 병소는 조영증강 초음파와 동적 조영증강 자기공명영상 운동 패턴 결과가 일치하였고 가중 카파 값 0.66으로 좋은 일치도를 나타냈다. 부분 군 분석에서 양성 병소는 우수한 일치를 보였고(가중 카파 값 = 0.84), 관내암종은 좋은 일치를 보였다(가중 카파 값 = 0.69).

결론 MRI에서 추가 검출된 유방 결절에 대한 조영증강 초음파의 진단 능력은 우수했다. 양성 및 관내암종 병소에서 동적 조영증강 자기공명영상과 조영증강 초음파의 운동 패턴 결과는 좋은 일치도를 보였다.

¹고려대학교 의과대학 고려대학교 구로병원 영상의학과,

²고려대학교 의과대학 고려대학교 안암병원 영상의학과,

³고려대학교 의과대학 고려대학교 안산병원 영상의학과,

⁴고려대학교 의과대학 의과학연구지원센터 고려대학교 구로병원 통계상담실